Eur. Phys. J. E (2012) **35**: 75
DOI 10.1140/epje/i2012-12075-0

THE EUROPEAN PHYSICAL JOURNAL E

Regular Article

Mimicking DNA stretching with the Static Mode method: Shear stress versus transverse pulling stress

M. Brut[1,2,a], A. Estève[1,3], G. Landa[1,3], and M. Djafari Rouhani[1,2]

[1] CNRS; LAAS; 7 avenue du colonel Roche, F-31077 Toulouse, France
[2] Université de Toulouse; UPS, LAAS; F-31077 Toulouse, France
[3] Université de Toulouse; LAAS; F-31077 Toulouse, France

Received 16 January 2012 and Received in final form 29 May 2012
Published online: 21 August 2012 –

Abstract. DNA sequencing using nanopores is closer than ever to become a reality, but further research and development still need to be done, especially to unravel the atomic-scale mechanisms of induced DNA stretching. At this level, molecular modeling and simulation are essential to investigate DNA conformational flexibility and its response to the forces involved. In this work, through a "Static Mode" approach, we present a directed exploration of the deformations of a 27-mer subjected to externally imposed forces, as it could be in a nanopore. We show how the DNA sugar-phosphate backbone undergoes the majority of the induced deformation, before the base pairing is affected, and to what extent unzipping initiation depends on the force direction.

1 Introduction

Translocation of biopolymers such as deoxyribonucleic acids (DNA), ribonucleic acids or polypeptides is an essential and ubiquitous biological process. *In vitro*, its study provides a great amount of information concerning the structure, the kinetics and the dynamics of such molecules [1–3]. During the last decade, the use of nanopores has offered an efficient and low-cost alternative to perform the translocation. In 1996, Kasianowicz *et al.* were the first to demonstrate how DNA molecules could be electrically driven through a α-hemolysin protein nanopore [4]. Since then, many teams have conducted such studies, using different nanopores, protein-based (α-hemolysin) or artificial (solid-state pores) [5–7]. Most of these studies focus on DNA, which has been intensively studied for the last 60 years for its versatile properties, first in biology, and then also for technological purposes [8]. In this context, the manipulation of single molecules has strongly grown in importance, and together with rapid development in detection, has opened new possibilities for high-speed and low-cost sequencing.

However, DNA sequencing using a nanopore device is a real challenge and has not yet been achieved [9–11]. Indeed, while the translocation mechanism of unstructured single-stranded DNA (ssDNA) is rather well understood [12–18], the lack of structural and dynamic information makes it difficult to elucidate the unzipping process by which a double-stranded DNA (dsDNA) separates and goes through the nanopore. While the unzipping is an essential step that needs to be harnessed, it is still poorly understood. More generally, the mechanical flexibility of DNA is a key element to understand its role in cellular functions and a convenient study case for polymer physics.

Recently, various experimental and numerical approaches have helped to understand how dsDNA, with a helix diameter larger than the pore size (respectively, 2.2 nm and 1.5 nm), could unzip. Their authors have shown that DNA unzipping is not only connected to the pore size [19], but to the sequence length and composition as well [20–22]. In these studies, mechanical micro or nanomanipulation were used, either to push DNA through the nanopore [19,20], or to force DNA unzipping [21,22]. Such single-molecule experiments have the advantage of providing mechanical information on DNA unzipping, since the strand separation is generated without a significant change of environment (pH, temperature, ...) [23]. Second, it is consistent with the idea that the unzipping process can be powered by an external force, as it is when DNA enters into a nanopore. In this approach, the two strands of a dsDNA molecule are pulled apart under the influence of a force, exerted with single molecule force spectroscopy techniques (optical tweezers, magnetic tweezers, AFM) [24] or micromechanical devices [25]. Theoretical models and numerical simulations have also emerged to test the elastic properties of DNA and the effects induced by pulling forces causing stretching and torsional stresses [26–33]. Based on polymer physics, numerical studies are a precious tool to interpret the experimental data and to predict structural

[a] e-mail: mbrut@laas.fr

changes. However, they provide no accurate information concerning the atomistic mechanisms involved.

In this work, we use the Static Mode method [34] to investigate how a mechanical action can lead to stretching the DNA structure. Based on the "induced-fit" concept [35], it allows the calculation of molecular deformations induced by external perturbations of specific molecular sites, in terms of force constants contained in the energy model. For this reason, this approach is well adapted for the atomic-scale treatment of macromolecular flexibility. One technical advantage is that it requires a very low computing cost, due to the harmonic approximation used in this method and to the resulting algorithm simplicity, which is roughly equivalent to a matrix inversion. In sect. 2.2, we discuss these aspects in more detail. Another technical advantage is that only one calculation is necessary for the determination of all the Static Modes, which are stored and can be reused in further applications, once calculated. They can be easily combined to simulate the molecular response to a designed stress, in this case, to stretch the dsDNA molecule. In the present article, we use customized perturbations to simulate deformations induced by local forces that could be exerted inside the nanopore. Our aim is to theoretically explore how DNA conformation is affected by various forces applied on the sugar-phosphate backbone in defined directions. We examine the tendency of dsDNA to separate and evaluate the most probable mechanical action inducing the strands' separation along with the atomistic mechanisms involved. With this model, the results are expected to depend on the structural organization of the double helix, and the manner in which the external forces are applied. We show how shear forces along the helical direction are absorbed by the flexible backbone without reaching the bases, and how transverse pulling forces can more likely lead to the dsDNA stretching with a tendency to initiate the base pair extension.

2 Materials and methods

2.1 Structures

A dsDNA was built using the NAB package [36] that provides a "perfect" canonical B-type DNA helix. We chose a 34-b strand, with the following random sequence: 5′-$G_{5'}$GCGACCTCGCGGGTTTTCGCTATTTATGAAAAT$_{3'}$-3′. Only the last 27 underlined nucleic acids are paired with a complementary strand. For the following, let us name A the 34-b strand and B the 27-b strand (see fig. 1). This structure was chosen in reference to Viasnoff *et al.* theoretical work [37] that uses a single-strand overhang threaded into the pore and allows us to simulate this case as well. Our structure was first subjected to a total energy minimization, using AMBER11 package [38] with an implicit solvent model and the ff99bsc0 force field [39]. This step is required to generate a conformation at the equilibrium and to extract the Hessian matrix. The matrix elements are then used to compute the Static Modes, as described in the following part.

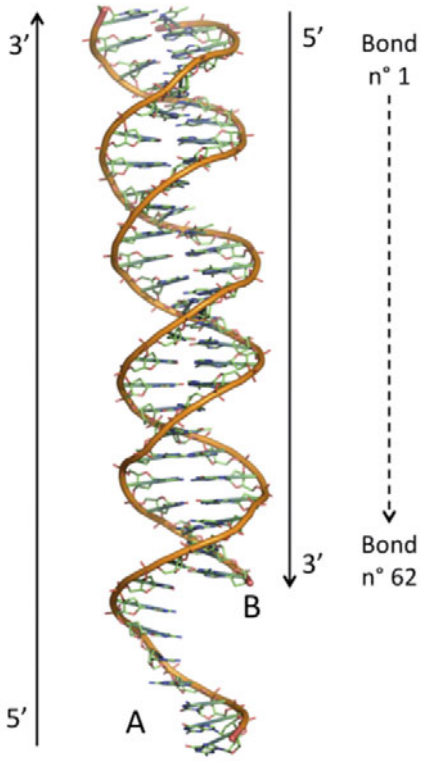

Fig. 1. Atomic representation of the dsDNA molecule, both strands A and B are shown. The inter-strand bond numbering is also indicated, from 1 to 62, in the 5′ → 3′ direction of strand B.

2.2 Static Mode calculation

Based on the optimized conformation, the Static Modes are then computed. Each of them represents the elementary molecular deformation resulting from the perturbation of a specific atom, in a specific direction x, y, z of the Cartesian space (see refs. [34,40–42] for more detail and discussion). The systematic calculation of the Static Modes implied by the application of a normalized force can be easily performed by the successive solicitation of each Hessian matrix line, when solving a linear set of equations. In the present version of the algorithm, the harmonic approximation greatly simplifies the problem since the energy landscape is totally defined by the Hessian matrix. However, it remains only valid for small deviations around equilibrium conformations. Therefore, in the following, we do not address the questions of total unzipping of the DNA strands, and certainly not those related to the DNA melting, which implies considering temperature effects. Rather, we examine which type of forces induces the largest deformations capable of starting the unzipping process. We consider stationary mechanical, electrostatic or optical forces, as used in experiments [24,25], and not random type forces, more typical of temperature effects. The calculations are valid at low temperatures, typically mimicking the output of single-molecule force-induced DNA unzipping experiments [20]. In particular, using Static Modes, we map local deformations of a dsDNA under local forces, investigate its flexibility, and also

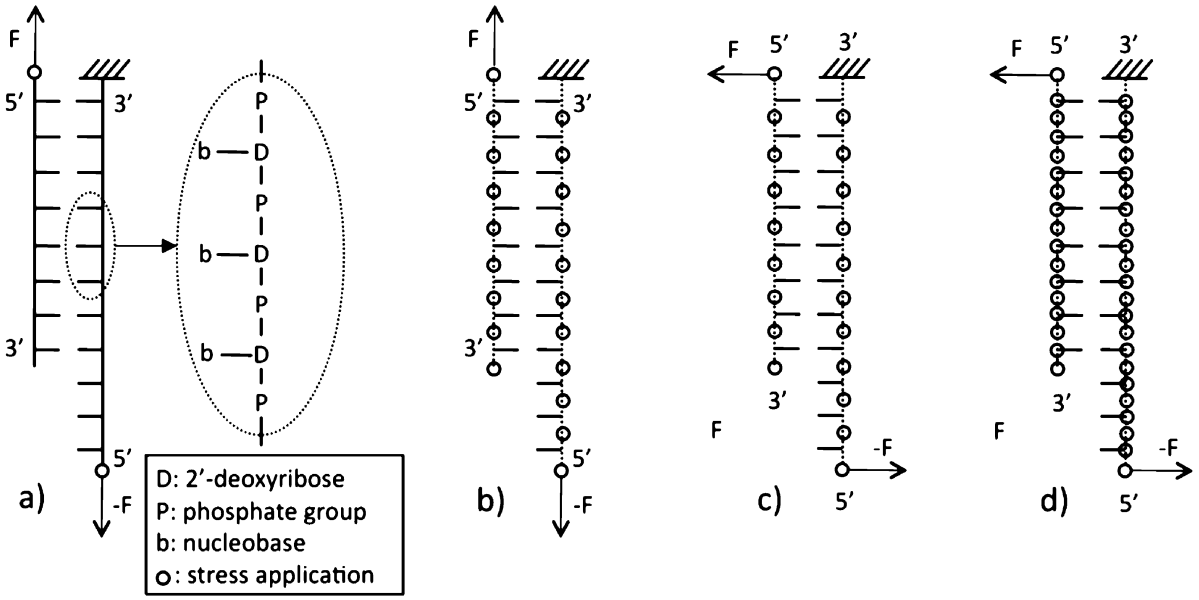

Fig. 2. Schematic representation of two types of stress application. On a), shearing forces are applied on the 5′-termini phosphate atoms, along the helical axis, in the $3' \rightarrow 5'$ direction. On b), the same forces are applied on each phosphate atom of the dsDNA molecule. c) Pulling forces are applied on each phosphate atom, along the transverse direction. d) The same transverse pulling forces are applied on each phosphate and each C4 atom. For a better readability, the force application points are localized with circles.

observe how the unzipping may locally start. All calculations are performed on dsDNA, which is in a stable conformation at room temperature and does not show multiple conformations. Because of the stationary nature of applied forces, the calculated local deformations lead to real new equilibrium configurations, which are no more temporary configurations reached during each oscillation cycle. However, they do not necessarily lead to the total unzipping of dsDNA.

The total unzipping can only occur by multiplication of the applied forces. That is the reason why we suggest, in the next section, several set of forces.

For this dsDNA molecule (1905 atoms), the calculation of all the Static Modes requires 50 min of CPU time (2.8 GHz Intel dual core processor). Once calculated, Static Modes are stored in a matrix $[M]$ ($3N \times 3N$-6) and can be directly used in a post-treatment procedure to explore the consequences of one or more external forces defined by the operator.

2.3 Force application

In the present work, the post-treatment consists in the direct application of local forces to pull apart the DNA strands. With the aim of exploring the structural changes, the A strand 3′-terminus is kept fixed, while normalized forces (that is, with the same intensity, set to 1) are exerted along the sugar-phosphate backbone in various directions. Using normalized force ($1\,\mathrm{eV/\AA^2}$) will result in small deformation but allows to qualitatively and quantitatively compare the effects of the force direction.

To apply a force $\vec{F}$ on the atom N_0, a matrix m_{N_0} ($3N \times 3$) is extracted from the Static Mode matrix $[M]$. m_{N_0} contains the atomic displacements resulting from the application of three elementary forces in the x, y, z directions, on the atom N_0. The molecular deformation field $\Delta\vec{X}$ induced by the application of the force $\vec{F}$ on N_0 is then directly deduced from the formula $\Delta\vec{X} = m_{N_0}\vec{F}$. Inter-strand distances are measured before and after deformation to characterize the base pair stretching induced by the force. As many forces as needed can be applied, the resulting global deformation being easily computed by a succession of linear combinations of the appropriate Static Modes. 62 canonical hydrogen bonds have been counted between base pairs. They are numbered from 1 to 62, following the base order, in the B strand $5' \rightarrow 3'$ direction (see fig. 1).

Four cases are presented in this article. The dsDNA molecule is successively stretched by applying shearing and transverse pulling forces on the sugar-phosphate backbone: a) on the phosphate atoms localized at the 5′-termini of the A and B strands, along the $3' \rightarrow 5'$ helical axis direction; b) on all the phosphate atoms of both strands, along the $3' \rightarrow 5'$ helical axis direction; c) on all the phosphate atoms in the transverse direction; d) on all the phosphate and C4 atoms in the transverse direction (see fig. 2). More detail together with the deformation resulting deformation are presented in the following section.

3 Results and discussion

3.1 Shearing forces on the 5′-extremities along the helical axis direction

As shown on fig. 2a, two forces are applied on the phosphate atoms situated at the A and B strand 5′-termini,

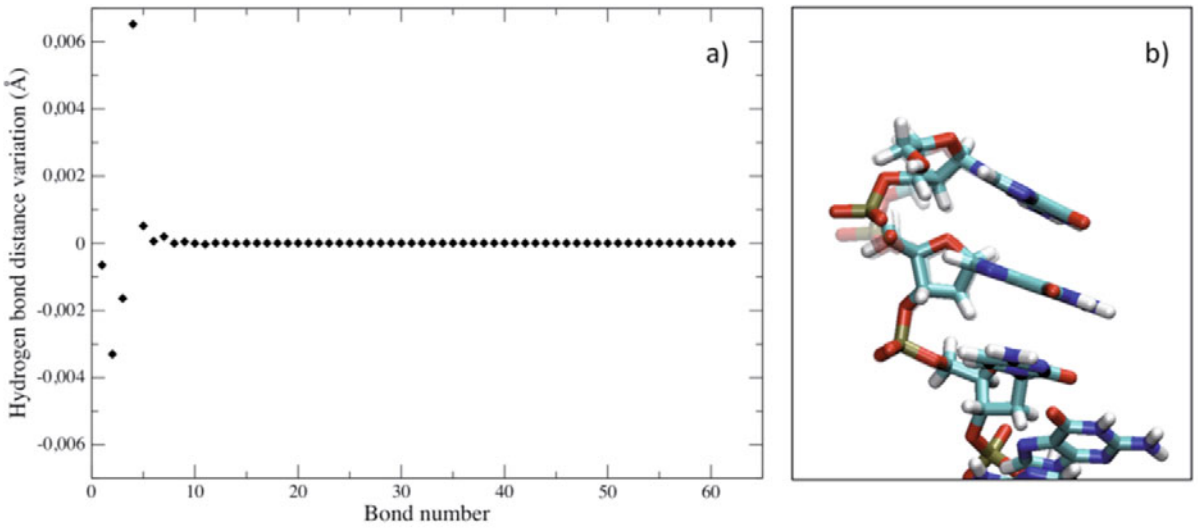

Fig. 3. Deformed structure resulting from a stress applied on the strand 5′-extremities, along the helical axis, in the $3' \rightarrow 5'$ direction (case shown on fig. 2a). Variations of the hydrogen bond length are given on graph a). An atomic representation of the A strand 5′-terminus is show on b). The deformation mainly affects the backbone and does not propagate further than the third nucleic acid.

Table 1. First four nucleic acids of the A strand (5′-terminus). Respectively, for the initial structure and the deformed structure obtained with a shearing force applied on the 5′-extremities, along the helical axis, in the 3′5′ direction (case shown on fig. 2a): phase angle, maximum amplitude of puckering, χ and γ torsion angle, and type of sugars 1, 2, 3, 4.

	Initial structure				Deformed structure			
	P	ν max	χ	γ	P	ν max	χ	γ
1	19.14	37.19	−156.84	58.74	26.21	40.21	−159.24	66.44
2	10.26	36.16	−154.60	58.11	2.08	30.52	−157.08	69.94
3	16.69	40.22	−150.79	57.13	17.16	40.28	−150.81	58.62
4	144.85	41.25	−98.54	57.44	144.85	41.25	−98.54	57.38

Table 2. First four nucleic acids of the B strand (5′-terminus). Respectively, for the initial structure and the deformed structure obtained with a shearing force applied on the 5′-extremities, along the helical axis, in the 3′5′ direction (case shown on fig. 2a): phase angle, maximum amplitude of puckering, χ and γ torsion angle, and type of sugars 1, 2, 3, 4.

	Initial structure				Deformed structure			
	P	ν max	χ	γ	P	ν max	χ	γ
1	154.65	36.68	−118.06	56.90	143.16	34.96	−119.01	54.52
2	124.60	37.60	−121.70	56.06	133.07	37.06	−124.26	61.00
3	129.17	39.79	−107.30	58.53	129.10	39.81	−107.34	59.13
4	130.37	37.13	−120.51	60.49	130.37	37.13	−120.51	60.52

along the helical axis, in the $3' \rightarrow 5'$ direction. The resulting stretching of each hydrogen bond between base pairs is presented on fig. 3a. Only the first five bonds, which belong to the first two base pairs, are affected. Induced variations are very small but still result from normalized forces. Since they are treated in the frame of a linear model, a coefficient higher than 1 can be attributed to these forces to get a proportional deformation, but here, small amplitudes do not affect our qualitative conclusions on the deformation characteristics. As seen in fig. 3b, this induced deformation is extremely local. It does not propagate further than the third following nucleic acid and has a significant impact on the backbone over a distance of 15 Å, while the bases are almost not displaced. The deformation propagates along the backbone and is absorbed through a sugar accommodation mechanism: sugar phase changes [43] and χ, γ torsion angles are presented in tables 1, 2 and 3 (according to IUPAC recommendations [44], χ and γ describe

Table 3. Last four nucleic acids of the A strand (3′-terminus). Respectively, for the initial structure and the deformed structure obtained with a shearing force applied on the 5′-extremities, along the helical axis, in the 3′5′ direction (case shown on fig. 2a): phase angle, maximum amplitude of puckering, χ and γ torsion angle, and type of sugars 1, 2, 3, 4.

	Initial structure				Deformed structure			
	P	ν max	χ	γ	P	ν max	χ	γ
1	166.37	35.09	−103.25	62.86	166.37	35.09	−103.25	62.86
2	152.22	40.60	−103.47	57.66	152.22	40.60	−103.47	57.66
3	157.62	35.16	−118.18	64.17	152.62	35.16	−118.18	64.17
4	137.71	41.15	−133.83	61.06	137.71	41.15	−133.83	61.06

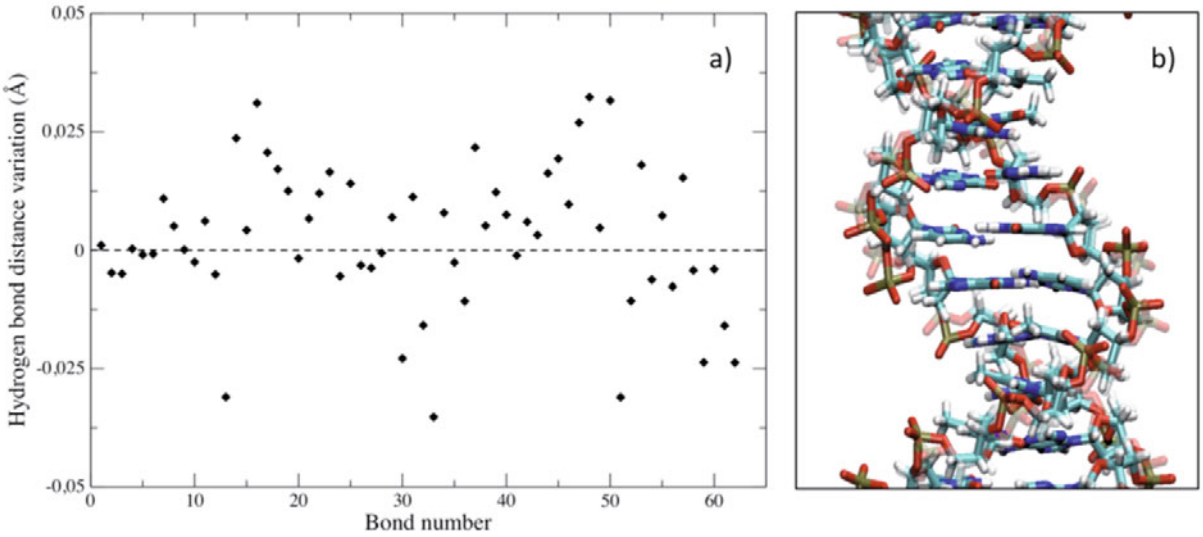

Fig. 4. Deformed structure resulting from a stress applied on each phosphate atom, along the helical axis, in the 3′ → 5′ direction (case shown on fig. 2b). Variations of the hydrogen bond length are given on graph a). An atomic representation of the medium part of the helix is show on b).

the sugar to base and phosphate to sugar torsion angles, respectively). In these tables, data concern, respectively, the first four nucleic acids of the A strand (5′-terminus), of the B strand (5′-terminus), and the last four nucleic acids of the A strand (3′-terminus). The results indicate that the A strand 3′-terminus is absolutely not affected by the stress imposed on the complementary B strand 5′-terminus (see table 3), which is explained by the fact that the bases are not reached by the deformation. In this case, a single force application is not sufficient to overcome the stability generated by inter-strand interactions. However, this first calculation allows an accurate investigation of a DNA strand response to a local phosphate stress, and beyond, the comparison of its characteristics depending on its state: bound or unbound to its complementary strand. Tables 1 and 2 bring information about the backbone accommodation at the 5′-extremities: the deformation is clearly visible on the stressed nucleic acid and its first neighbor, it propagates to the second neighbor in the overhang, but none of the values is affected from the fourth neighbor. In comparison, the B strand 5′-extremity is more rigid. In particular, γ variations, which represent the sugar motion with respect to the phosphate, are more important in the overhang, with amplitudes reaching 12°, instead of 5° in the duplex. However, in the case of the double strand (B strand 5′-terminus), sugar phase values are affected to a larger extent, with amplitudes reaching 12° (P varies from 154.65° to 143.16°, and from 124.60° to 133.07° for sugars 1 and 2). Remarkably the backbone accommodation is not the same in both cases. In the double strand, more constrained, the backbone is rigidified, while sugars undergo larger modifications. They act like pivots between the backbone and the rigid base pair stacking, stabilized by both van der Waals forces and π-stacking, which result in small χ variations (around 2.5°). The potential role of the energy model in this result has already been discussed in previous work [43]. In this calculation, the applied force is not strong enough to prevail upon base stacking and base pair interaction. In the following, we increase the number of applied forces.

3.2 Shearing forces on all phosphate atoms along the helical axis direction

Again, shearing forces are applied along the helical axis, in the 3′ → 5′ direction, but on all phosphate atoms of the molecule. The resulting deformation is shown on fig. 4b.

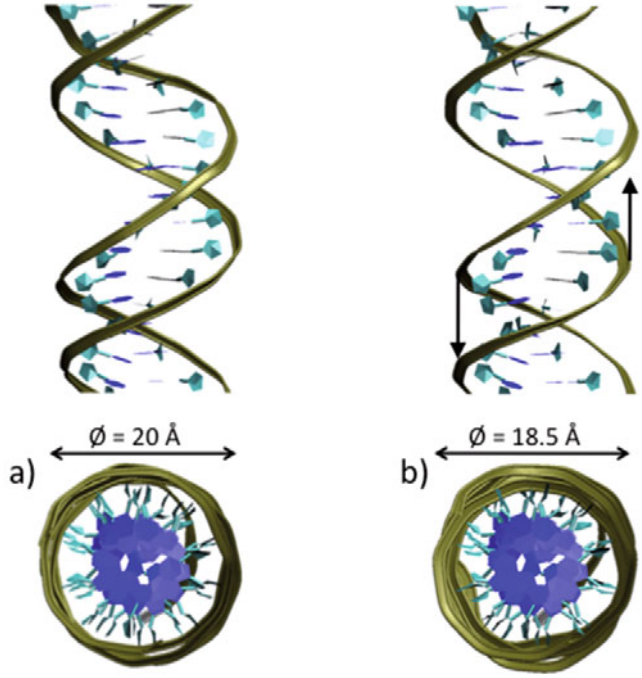

Fig. 5. On the left, longitudinal and transverse views of the initial helical structure. On the right, corresponding views of the deformed structure resulting from a stress applied on the each phosphate atom, along the helical axis, in the $3' \rightarrow 5'$ direction (case shown on fig. 2b).

In this case too, the deformation propagates along the backbone and is lost to a large extent before reaching the bases. But due to the large number of applied forces, all hydrogen bonds present more significant length variations. Amplitudes are not heterogeneous, most of them range between -0.010 and 0.025 Å, but the largest ones reach $|0.035$ Å$|$ (see fig. 4a). Some values are around or below 0, which can be explained by the three-dimensional structure of the duplex: this type of force may alternately open or close the hydrogen bonds. As shown on fig. 5, the shearing forces applied along the helical axis induce its longitudinal stretching. Most of the time, this mechanism lightly extends the hydrogen bonds, but sometimes, depending on the base orientation, it can contribute to their contraction.

3.3 Pulling forces on all phosphate atoms along the transverse direction

In this calculation, new forces are applied on all phosphate atoms, along the "transverse direction". Here, we define this direction as the axis connecting each phosphate atom and the associated phosphate atom of the complementary nucleic acid. On each pair of phosphate atoms, a couple of forces is applied, to create a stretching force, pointing outward from the duplex (see fig. 2c). In other words, the duplex is stretched in the base plane. The induced deformation is shown on fig. 6b. Considering the hydrogen bond stretching presented on fig. 6a, a first remark can be made concerning the amplitudes, with maxima reaching four times the values found in the previous calculation. Second, while the deformations were previously spread on both positive and negative sides, almost all the values are positive in this case In these conditions, applying a transverse stress is much more efficient to stretch the base pairs. On fig. 7b, one can clearly see that the helix diameter gets larger with the stress. However, again, the inter-base stretching is smaller than we could expect because of the sugar accommodation. This calculation highlights again the crucial role played by sugars that absorb the strain imposed on the backbone (shown on fig. 6b).

3.4 Transverse pulling forces on the phosphate and C4′ atoms

In the last simulation, we apply the same transversal stress on the phosphate atoms, but also on all the C4′ atoms, belonging to the sugar rings. In this calculation, we speculate that this force will be too strong to be absorbed by the sugars and should reach the bases more efficiently. The deformations are qualitatively similar to those obtained previously, but with amplitudes twice as large as with forces applied on phosphate atoms only (see fig. 8a); stretching values reach 0.4 Å Multiplying the number of applied forces allows us to enhance the stretching mechanism. It is clearly visible on fig. 8b that the bases do not move in their plane, the backbone torsional accommodation induces a sugar phase change, which induces itself a rotation of the bases. This process also explains the amplitude disparity: the bases rotating in relation to each other, some hydrogen bonds break before others.

4 Conclusion

In this paper, we show how the Static Mode method can be used to design any type of force in order to distort a molecule, and in this case, to explore a dsDNA response to conformational stress. In these preliminary calculations, external forces are normalized, which explains the small deformation amplitudes we get. However, since they are treated in the frame of a linear model, a coefficient higher than 1 can be easily attributed to these forces to induce a proportional deformation. In this frame, these exploratory calculations provide useful qualitative information and open the way for further investigation, using more complex forces, traducing a more complex and realistic environment. Following recent experiments and calculations using stretching forces to investigate the unzipping mechanism, we show how our approach can provide further insights into the relation existing between local backbone perturbations and the absorption/propagation mechanism of the deformation. In particular, we analyze the effects of two kinds of stresses, via shearing and transverse pulling forces applied on the backbone, respectively, along the helical and transverse directions. In the first case, when opposite forces are applied along the helical axis, interstrand distances present very small variations, while the

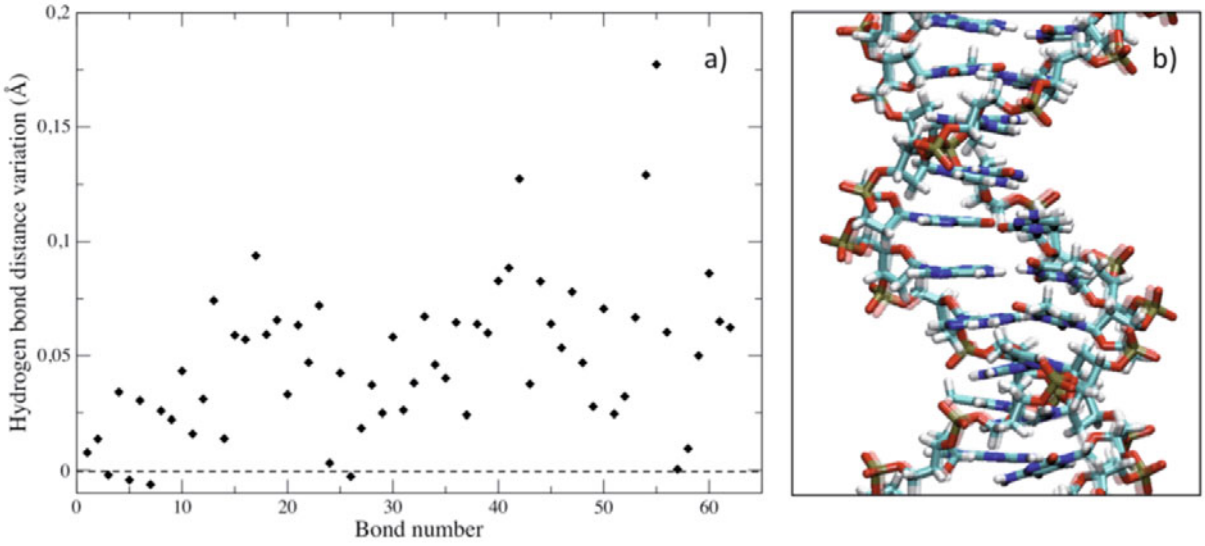

Fig. 6. Deformed structure resulting from a stress applied on each phosphate atom, along the transverse axis and pointing outward the duplex (case shown on fig. 2c). Variation of the hydrogen bond length are given on graph a). An atomic representation of the medium part of the helix is show on b).

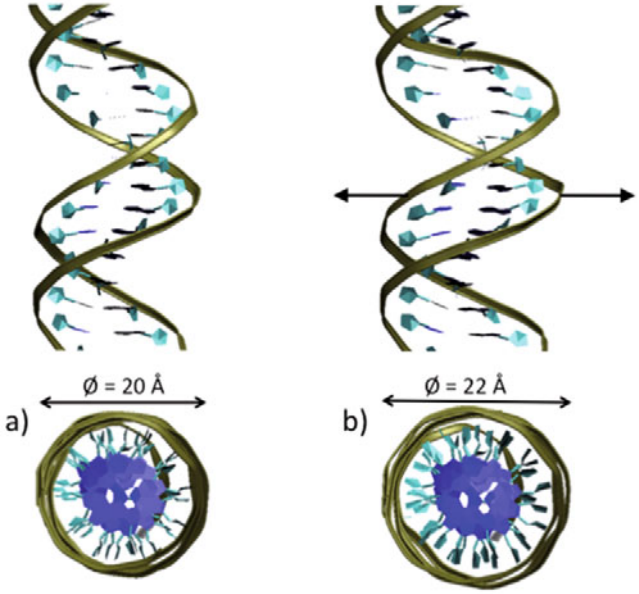

Fig. 7. On the left, longitudinal and transverse views of the initial helical structure. On the right, corresponding views of the deformed structure resulting from a stress applied on the each phosphate atom, along the transverse axis and pointing outward the duplex (case shown on fig. 2c).

sugar-phosphate backbone undergoes significant deformations. The backbone is highly flexible, contrary to the base stacking that exhibits a strong stiffness due to inter and intra-strand base interactions. This result is not surprising, since it has been experimentally demonstrated that, with such shearing forces, a high force regime is necessary to unzip the duplex. Large forces are required to overcome the short-range base pair stacking interactions that we observe and that make the formation of overstretched DNA difficult [45]. Below this regime, it has been shown that the dsDNA molecule can be overstretched about 1.7 times. Our calculations show a similar behavior. More, our observations corroborate theoretical results previously pointed out [46]: before the unzipping occurs, the shearing stress relaxes locally (along about 5 base pairs) along the backbone, while other base pairs experience no shear force. However, according to our pulling force calculations, it appears much more favorable to extent the base pairs with a transverse stress. In this case too, the backbone undergoes a significant accommodation, nevertheless, the sugar puckering induces a base rotation that leads to a possible hydrogen bond breaking.

In summary, we have presented an original approach aimed at evaluating a dsDNA response to customized shearing and transverse pulling forces. The next step to complete this study is to introduce anharmonic effects in the calculations. This can be performed either by the use of empirical force constants, not derived from the Hessian matrix but from transitions states, or through the conversion of Cartesian coordinates to generalized torsion coordinates. The second approach, presently under investigation, will allow a quantitative comparison of our results with those cited in the literature. We think that these calculations can further the understanding of the unzipping process occurring in single-molecule force experiments. This knowledge is particularly important at a moment of growing interest for the challenging single-molecule manipulation.

This work was supported by the French National Agency for Research (ANR-VIBBnano) and the European COST project (Bio-integrated technologies). We thank the CALMIP Supercomputer Center for CPU resources. We also wish to thank Virgile Viasnoff from ESPCI - UMR CNRS Gulliver for helpful discussions.

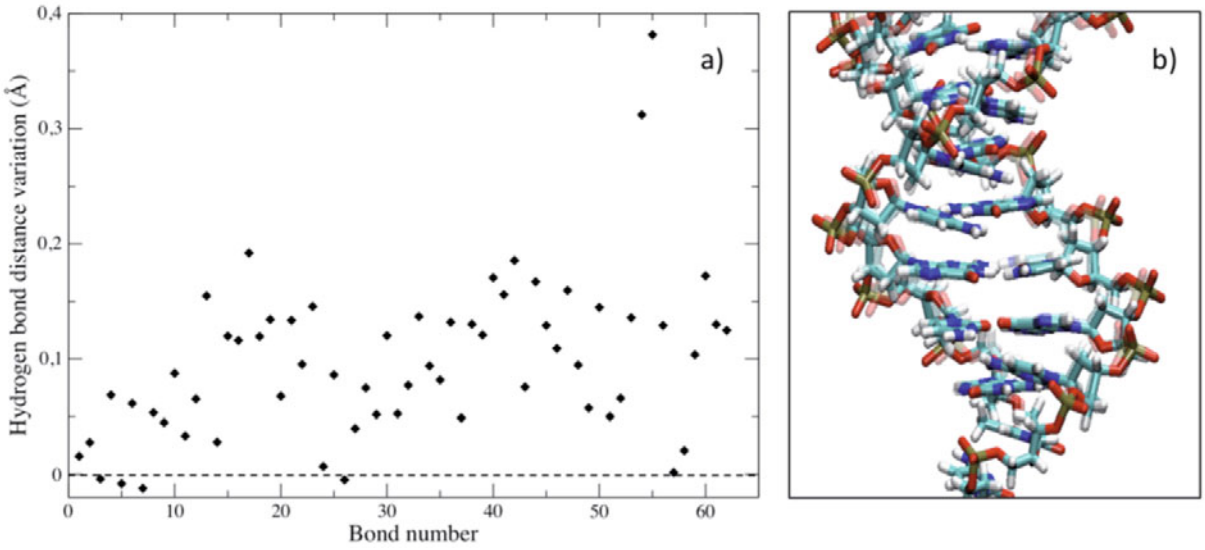

Fig. 8. Deformed structure resulting from a stress applied on the each phosphate and C4′ atom, along the transverse axis and pointing outward the duplex (case shown on fig. 2d). Variations of the hydrogen bond length are given on graph a). An atomic representation of the medium part of the helix is show on b).

References

1. U.F. Keyser, J. R. Soc. Interface **8**, 1369 (2011).
2. C.R. Martin, Z.S. Siwy, Science **317**, 331 (2007).
3. M. Muthukumar, J. Chem. Phys. **111**, 10371 (1999).
4. J.J. Kasianowicz, E. Brandin, D. Branton, D.W. Deamer, Proc. Natl. Acad. Sci. U.S.A. **93**, 13770 (1996).
5. A.J. Storm, J.F. Chen, H.W. Zandbergen, C. Dekker, Phys. Rev. E **71**, 051903 (2005).
6. T. Osaki, J.P. Barbot, R. Kawano, H. Sasaki, O. Français, B. Le Pioufle, S. Takeuchi, Procedia Engin. **5**, 796 (2010).
7. A. Han, G. Schürmann, G. Mondin, R.A. Bitterli, N.G. Hegelbach, N.F. de Rooij, U. Staufer, Appl. Phys. Lett. **88**, 093901 (2006).
8. N.C. Seeman, Mol. Biotechnol. **37**, 246 (2007).
9. D. Branton, D.W. Deamer, A. Marziali, H. Bayley, S.A. Benner, T. Butler, M. Di Ventra, S. Garaj, A. Hibbs, X. Huang, S.B. Jovanovich, P.S. Krstic, S. Lindsay, X.S. Ling, C.H. Mastrangelo, A. Meller, J.S. Oliver, Y.V. Pershin, J.M. Ramsey, R. Riehn, G.V. Soni, V. Tabard-Cossa, M. Wanunu, M. Wiggin, J.A. Schloss, Natl. Biotechnol. **26**, 1146 (2008).
10. J.J. Nakane, M. Akeson, A. Marziali, J. Phys.: Condens. Matter **15**, 1365 (2003).
11. U. Mirsaidov, J. Comer, V. Dimitrov, A. Aksimentiev, G. Timp, Nanotechnology **21**, 395501 (2010).
12. D.K. Lubensky, D.R. Nelson, Biophys. J. **77**, 1824 (1999).
13. P.G. De Gennes, Proc. Natl. Acad. Sci. U.S.A. **96**, 7262 (1999).
14. P.J. Bond, A.T. Guy, A.J. Heron, H. Bayley, S. Khalid, Biochemistry **50**, 3777 (2001).
15. O. Flomenbom, J. Klafter, Phys. Rev. E **68**, 041910 (2003).
16. M.G. Fyta, S. Melchionna, E. Kaxiras, S. Succi, Multiscale Model. Simul. **5**, 1156 (2006).
17. C. Forrey, M. Muthukumar, J. Chem. Phys. **127**, 015102 (2007).
18. K. Luo, T. Ala-Nissila, S-C. Ying, A. Bhattacharya, Phys. Rev. Lett. **100**, 050901 (2008).
19. J. Comer, V. Dimitrov, Q. Zhao, G. Timp, A. Aksimentiev, Biophys. J. **96**, 593 (2009).
20. U. Bockelmann, Ph. Thomen, B. Essevaz-Roulet, V. Viasnoff, F. Heslot, Biophys. J. **82**, 1537 (2002).
21. B. McNally, M. Wanunu, A. Meller, Nano Lett. **8**, 3418 (2008).
22. V. Viasnoff, N. Chiaruttini, U. Bockelmann, Eur. Biophys. J. **38**, 263 (2009).
23. R. Kapri, S.M. Bhattacharjee, J. Phys.: Condens. Matter **18**, S215 (2006).
24. R. Lavery, A. Lebrun, J.-F. Allemand, D. Bensimon, V. Croquette, J. Phys.: Condens. Matter **14**, 383 (2002).
25. B. Essevaz-Roulet, U. Bockelmann, F. Heslot, Proc. Natl. Acad. Sci. U.S.A. **94**, 11935 (1997).
26. B. Chakrabarti, D.R. Nelson, J. Phys. Chem. B **113**, 3831 (2009).
27. C. Barbieri, S. Cocco, R. Monasson, F. Zamponi, Phys. Biol. **6**, 025003 (2009).
28. P.M. Lam, L. Zhen, J. Stat. Mech. P06023 (2011).
29. J.Z.Y. Chen, Phys. Rev. E **66**, 031912 (2002).
30. D.K. Lubensky, D.R. Nelson, Phys. Rev. E **65**, 031917 (2002).
31. Y. Kafri, D. Mukamel, L. Peliti, Eur. Phys. J. B **27**, 135 (2001).
32. N. Singh, Y. Singh, Eur. Phys. J. E **17**, 7 (2005).
33. A.R. Singh, D. Giri, S. Kumar, J. Chem. Phys. **132**, 235105 (2010).
34. M. Brut, A. Estève, G. Landa, G. Renvez, M. Djafari Rouhani, Eur. Phys. J. E **28**, 17 (2009).
35. G.G. Hammes, Y-C. Chang, T.G. Oas, Proc. Natl. Acad. Sci. U.S.A. **106**, 13737 (2009).
36. T. Macke, D.A. Case, *Molecular modeling of nucleic acids* (American Chemical Society, Washington, D.C., 1998).
37. U. Bockelmann, V. Viasnoff, Biophys. J. **94**, 2716 (2008).
38. D.A. Case, T.A. Darden, T.E. Cheatham, C.L. Simmerling, J. Wang, R.E. Duke, R. Luo, R.C. Walker, W. Zhang, K.M. Merz, B. Wang, S. Hayik, A. Roitberg, G. Seabra, I. Kolossvary, K.F. Wong, F. Paesani, J. Vanicek, L. Jian,

X. Wu, S.R. Brozell, T. Steinbrecher, H. Gohlke, Q. Cai, X. Ye, J. Wang, M-J. Hsieh, V. Hornak, G. Cui, D.R. Roe, D.H. Mathews, M.G. Seetin, C. Sagui, V. Babin, T. Luchko, S. Gusarov, A. Kovalenko, P.A. Kollman, B.P. Roberts, *AMBER 11* (University of California, San Francisco, 2010).
39. A. Perez, I. Marchan, D. Svozil, J. Sponer, T.E. Cheatham, C.A. Laughton, M. Orozco, Biophys. J. **92**, 3817 (2007).
40. M. Brut, A. Estève, G. Landa, G. Renvez, M. Djafari Rouhani, D. Gauchard, Tetrahedron **66**, 9123 (2010).
41. M. Brut, A. Estève, G. Landa, G. Renvez, M. Djafari Rouhani, J. Phys. Chem. B **115**, 1616 (2010).
42. M. Brut, A. Estève, G. Landa, M. Djafari Rouhani, M. Vaisset, D. Gauchard, Mater. Sci. Eng. **169**, 23 (2010).
43. C. Altona, M. Sundaralingam, J. Am. Chem. Soc. **94**, 8205 (1972).
44. IUPAC-IUB Commission on Biochemical Nomenclature (CNB), Pure Appl. Chem. **40**, 291 (1974).
45. P. Cluzel, A. Lebrun, C. Heller, R. Lavery, J-L. Viovy, D. Chatenay, F. Caron, Science **271**, 792 (1996).
46. P.G. deGennes, C. R. Acad. Sci., Ser IV: Phys. **2**, 1505 (2001).